R-13-32

# Influence of local cold work in creep failure of phosphorus doped oxygen free copper

Karin Mannesson, Henrik CM Andersson-Östling,
Rolf Sandström

Swerea KIMAB

October 2013

**Svensk Kärnbränslehantering AB**
Swedish Nuclear Fuel
and Waste Management Co

Box 250, SE-101 24 Stockholm
Phone +46 8 459 84 00

ISSN 1402-3091
SKB R-13-32
ID 1400736

# Influence of local cold work in creep failure of phosphorus doped oxygen free copper

Karin Mannesson, Henrik CM Andersson-Östling,
Rolf Sandström

Swerea KIMAB

October 2013

# Abstract

In Sweden nuclear waste is planned to be encapsulated in cast iron inserts inside a sealed copper shell. The copper is subjected to handling that can induce cold work, for example through indentations during transport and handling.

Creep tests have been performed on 4 series with different indentation depths, including one series that was annealed after indentation. The material was oxygen free phosphorus doped copper and the creep tests were performed at 75°C in test rigs without loading arm.

The results show no significant effect on the creep rupture time and the creep ductility with size of indentation depth. Also the specimens annealed after indentations have a similar behaviour to the specimens without indentations.

# Contents

# 1 Introduction

In Sweden spent nuclear fuel from nuclear power plants are planned to be disposed by encapsulating in cast iron inserts inserted in a sealed copper shell. The cast iron acts as an inner load bearing and the copper shell protects against corrosion from the outside environment and also has a high ductility.

Both during manufacturing of the copper shell and the final deposition in the repository the copper is exposed to handling that can induce cold work in the material. Local indentations may arise from a tool and computations have shown that the local cold work can become very large (SKBdoc 1205273). Indentation by a flat cylindrical tool with a diameter of 20 mm has been estimated to give the following effects: indentations of 1.1 mm to 3.9 mm on a 50 mm thick plate gives cold work corresponding to 12% to 53% respectively. The corresponding stresses were 500 to 700 MPa, respectively (Andersson-Östling and Sandström 2009).

It is known that if 12 to 24% cold work is introduced the creep ductility is reduced but a ductility of about 10% or more still remains (Martinsson and Andersson-Östling 2009). One can expect that there is a gradual decrease in the ductility with increasing amount of cold work. From a design point of view as well as for the handling of the canisters it is of importance to know how fast and how large this decrease in ductility will be. The influence of cold work on creep ductility has so far been studied for uniaxial specimens with homogenous cold work. In an indentation situation the cold work may be quite inhomogeneous and this may affect the creep ductility.

This work aims to investigate the influence of cold work introduced by local indentations on the creep ductility.

# 2 Experimental

The material tested in this study is phosphorus doped, oxygen free copper (Cu-OFP). The specimens were taken from the part of the extruded tube T48-R2 corresponding to the bottom part of the ingot. The chemical composition of the material is presented in Table 2-1 (SKB 2010). Specimens with a rectangular cross section, see Figure 2-1, were manufactured and annealed in 600°C for 5 minutes followed by salt water quenching to remove all cold work introduced during machining. The rectangular cross section was used to make the indentation step more controlled, and also to allow for part of the cross sectional area where the indentation is placed to remain undeformed. In total five test series were included. One test series was made without indentation since the cross section has not been tested before. Three different indentation depths were used and also one test series was annealed both before and after indentation.

- Annealed, no indentation.
- Annealed, 1 mm indentation.
- Annealed, 1.5 mm indentation.
- Annealed, 2 mm indentation.
- Annealed, 2 mm indentation then annealed again.

The indentations were performed in a Schenk-Trebel RM 100 using a conical indentation body of hardened steel. The angle was 45°, see Figure 2-2, and the indentation speed was set to 3 mm/min. The specimens were placed with the parallel length on a flat surface with the ends hanging free to make sure that the specimens were not bent. See Figure 2-3 for setup of the test procedure. The indentation depths were measured using stereo microscope to assure that the correct depths were achieved. Other indenter geometries, such as cylindrical and spherical geometries, will be tested in a future work. These geometries will give plastic strains of a lower magnitude but distributed over larger areas, compared to the conical type, and could have greater influence on the specimens residual creep properties.

**Table 2-1. Chemical composition of material in ppm (SKB 2010).**

| Cu (%) | Pb | Bi | As | Sb | Sn | Zn | Mn | Cd |
|---|---|---|---|---|---|---|---|---|
| 99.99 | 0.27–0.28 | 0.119–0.120 | 0.82 | 0.06 | 0.06–0.07 | < 0.1 | < 0.1 | <0.003 |

| Fe | Ni | Ag | Se | Te | S | O | H | P |
|---|---|---|---|---|---|---|---|---|
| 1.4–1.5 | 0.8–0.9 | 13.4–13.5 | < 0.09 | 0.05 | 4.4 | 0.8–1.5 | 0.3–0.5 | 66–72 |

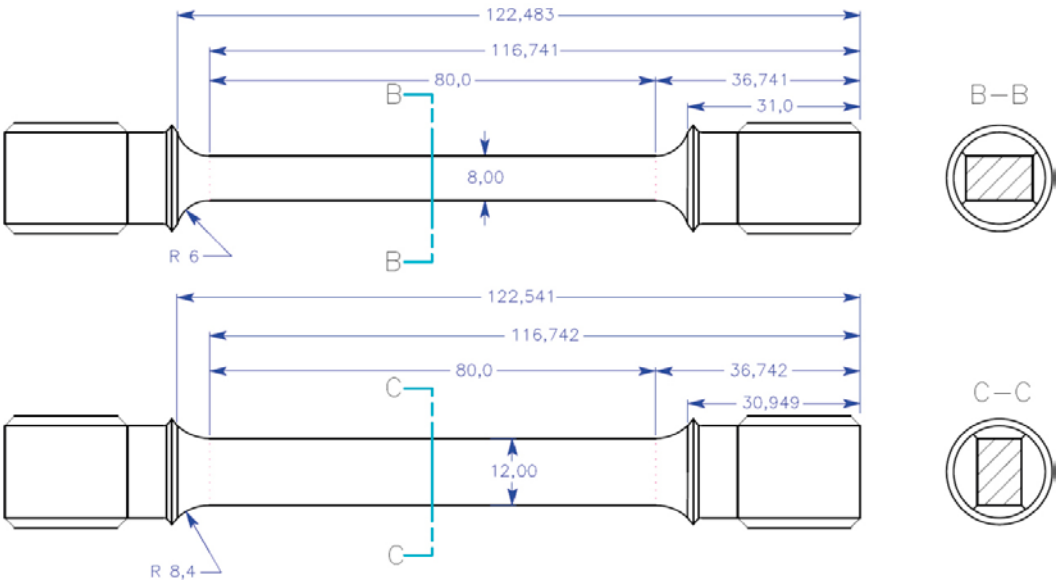


***Figure 2-1.*** *Drawing of creep specimen.*

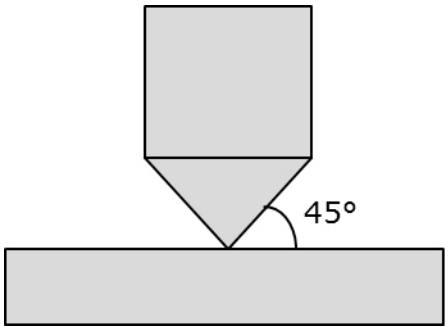


***Figure 2-2.*** *Drawing of the conical indentation body with angle to specimen indicated.*

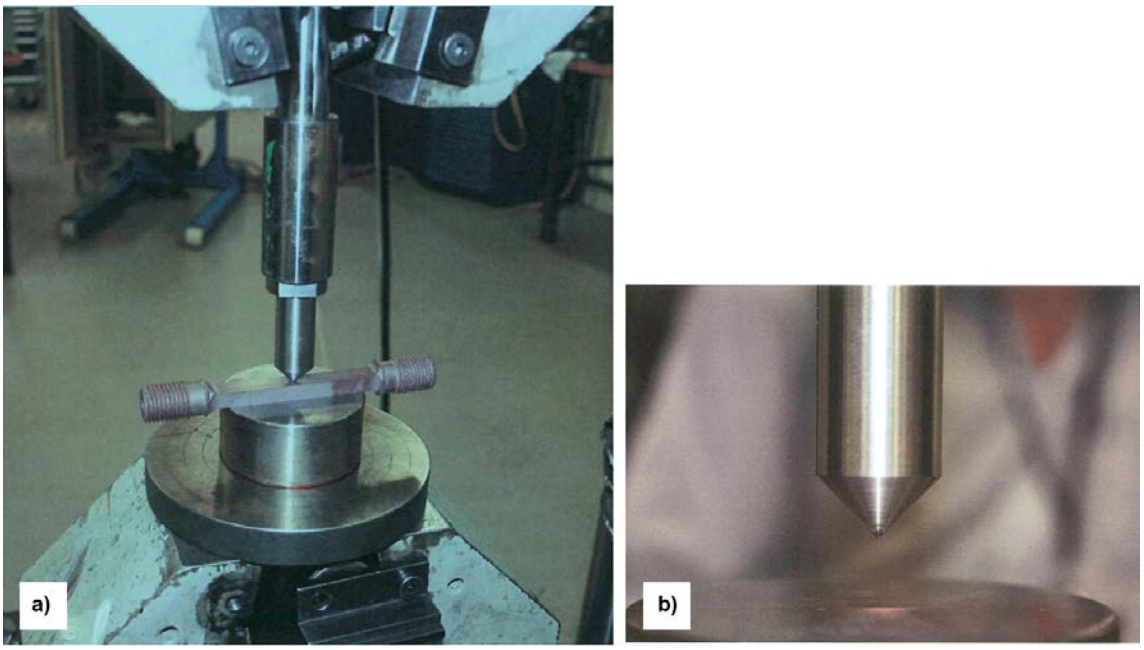


***Figure 2-3.*** *a) Specimen setup for indentations of Cu-specimens b) conical indentation body.*

After the indentations had been made iso-thermal creep tests were performed at 75°C. Four to five tests were performed for each set of creep series. The stress was chosen to give rupture times between 100 and 5,000 hours.

Creep test rigs without loading arms were used, Figure 2-4 and Figure 2-5. The loading arm has been replaced by a step motor actuating on the specimen through a gearbox and an angled gear. In the load line a load cell is incorporated and the step motor is controlled by feedback from the load cell. An in-house developed computer programme controls the test and allows for application of the load in a preset time. For calibration purposes the load cell is coupled to a calibration load cell before testing to ensure correct load. The load is applied linearly with time, and the longest application tested is 6 months. The load during the creep phase of the test is controlled to within 1 N. The furnace is of the hot air type and the temperature during the test is controlled to within ± 1°C. Since the strain of the specimen cannot be measured by extensometers attached to the specimen itself, the solution used was to measure strain outside the furnace. An extensometer was affixed to the load rod below the load cell and the strain measured to within 100 nm, Figure 2-4. Since the strain measured at this position includes strains in the load rods and the test rig itself, a phenomenon called the compliance of the test rig, this has to be compensated for. Before testing commenced a stiff dummy steel specimen was mounted in place of the copper specimen. The load was then applied to the test rig and the resulting strain was logged for each load increment. A compensating mathematical expression was obtained and this was then applied to the real tests yielding the correct strain on the specimen. When the load becomes constant also the machine compliance is also constant and therefore it is possible to measure the strain on the load rod. See Figure 2-5 for graph over machine compliance.

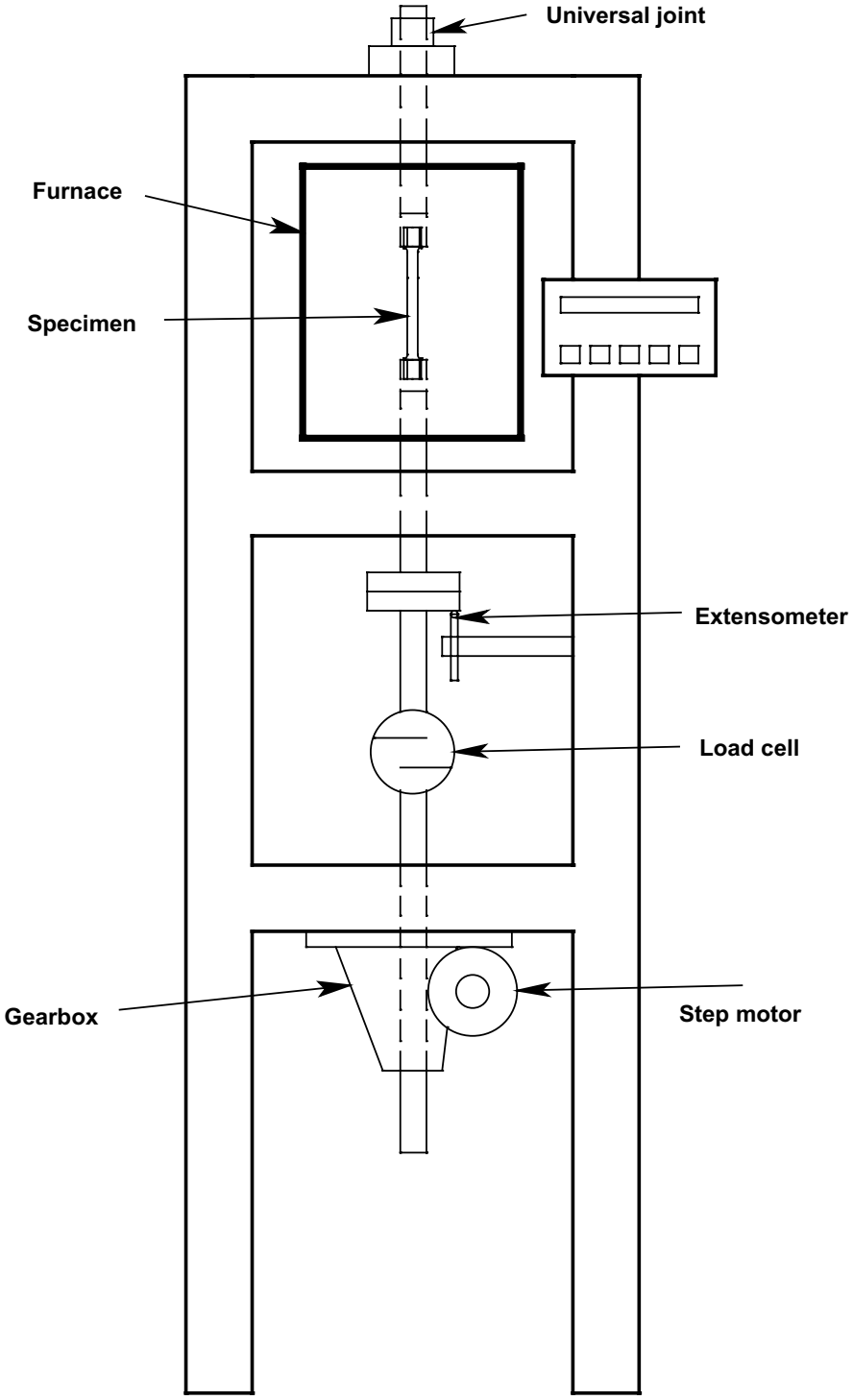


***Figure 2-4.*** *Schematic drawing of the load controlled creep test rig.*

When the test is started the specimen is placed inside the furnace and heated to the test temperature without any applied load. When the test temperature has been reached the specimen is allowed to rest for a few hours to guarantee that the temperature is stable before the load is applied. The accuracy of the load calibration is 10 N. The standard procedure is to apply the load stepwise and within 3 minutes from the start of the loading. During this initial loading the strain is measured and logged. Three thermocouples are attached to the specimen in order to measure and control the temperature. When full load is applied, the strain is measured continuously until fracture occurs.

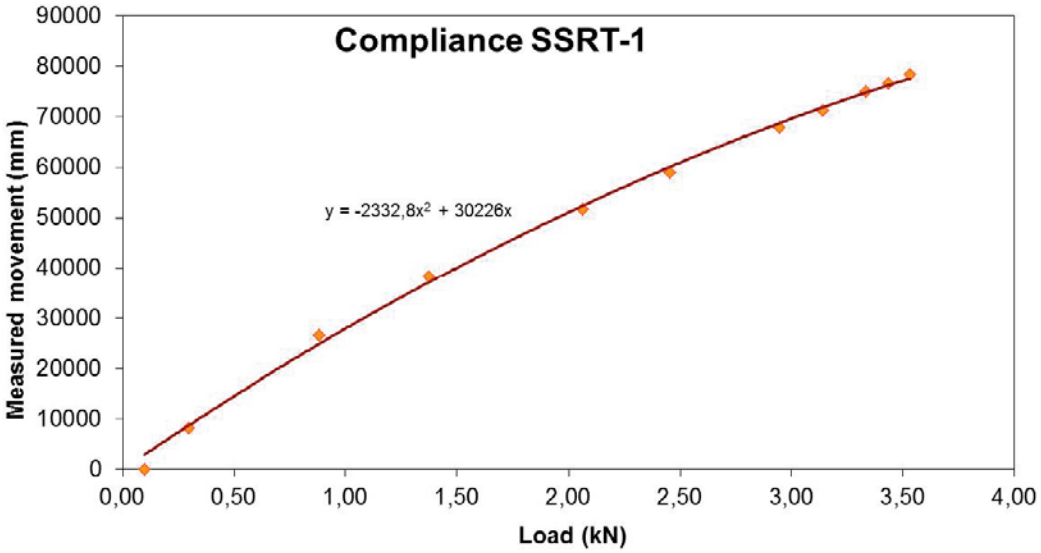


***Figure 2-5.*** *Graph over machine compliance in the test rig known as SSRT1.*


***Figure 2-6.*** *Image of the test rig in laboratory.*

In this study loading was performed in three steps, see Figure 2-7, since the maximum translational speed of the lower pull rod is slower than the creep rate during loading. The blue, filled line, curves corresponds to the three loading steps and the red, dashed line, to the creep. $F_w$ stands for the set load and $F_r$ for the real load during the loading operation. The loading steps proceed for approximately 7 minutes each, the last step starts approximately when 95% of the real load is reached. In this way the loading will be comparable for all test series.

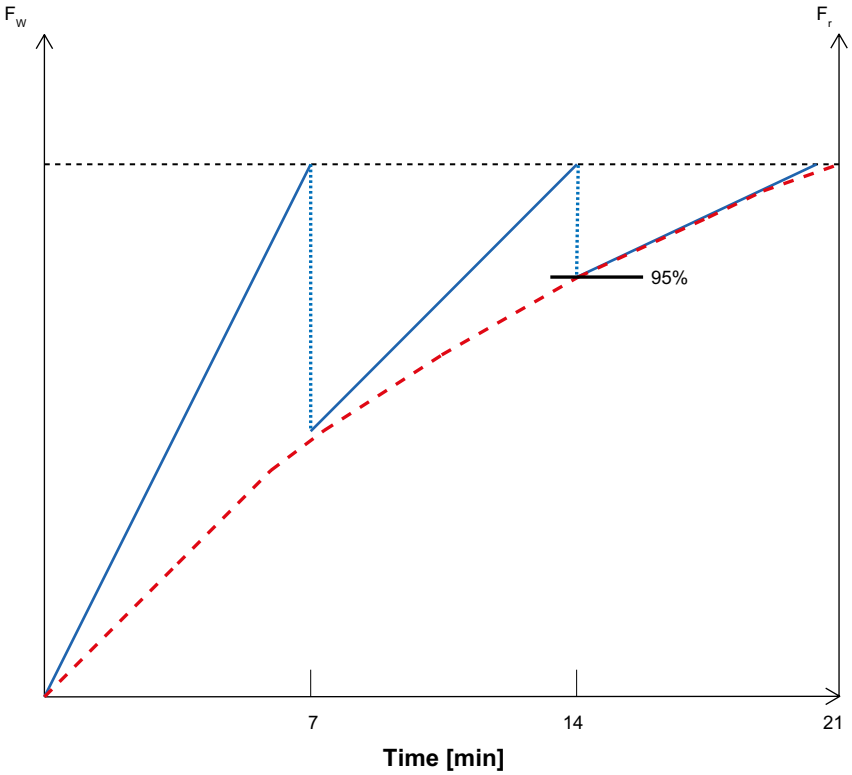


***Figure 2-7.*** *Loading scheme. Filled blue line corresponds to the three loading steps and dashed red line to the creep in the material. Fw is the set load and Fr is the real load.*

# 3 Results

## 3.1 Simulations

FEM-simulations of the indentation were made before the creep tests to select the appropriate test geometry. The simulations are limited in scope and used during the conduction of the test programme to prepare for the indentation phase. A more extensive modelling of the whole specimen during creep is needed for completeness, but was not included in the present work.

The FEM software Comsol 3.5a was used. A specimen with the same dimensions of the gauge length as in the creep specimens was chosen, Figure 2-1. These dimensions were 80×12×8 mm corresponding to the x-axis, z-axis, and y-axis, respectively. The mesh applied in the 3D-computation is illustrated in Figure 3-1.

Due to symmetry only half of the length and half of the width of the specimen were used in the FEM-modelling. Conical, cylindrical and spherical indenters were considered initially. However, very large local strains were obtained for cylindrical and spherical indenters, which were expected to be difficult to control experimentally. For this reason the work was concentrated to conical indenters, and no results are given here for the other types. The chosen geometry of the indenter (punch) was a cone with a height of 3 mm and a maximum radius of 1.5 mm. An elasto-plastic stress analysis was performed. The chosen flow rule can be found in Sandström and Hallgren (2012).

The resulting displacement of the material after applying the indenter is shown in Figure 3-2 and the resulting stresses and strains are given in Figure 3-3 and Figure 3-4.

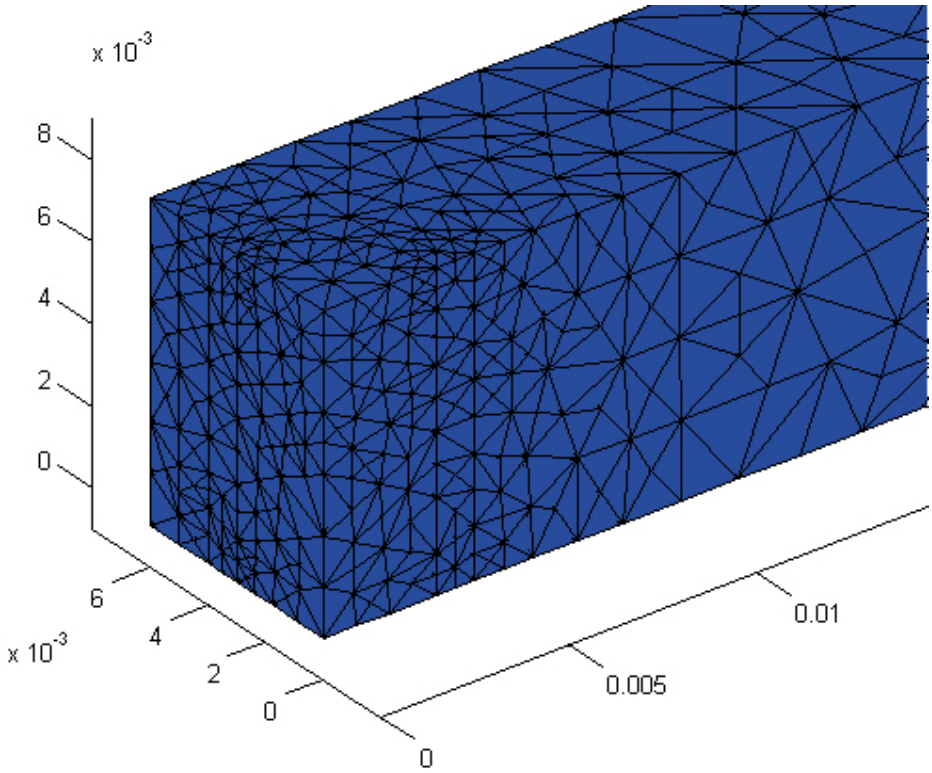


***Figure 3-1.*** *Mesh size in the simulated specimen. x-axis is along the specimen, y-axis in the width direction and z-axis in the vertical thickness direction.*

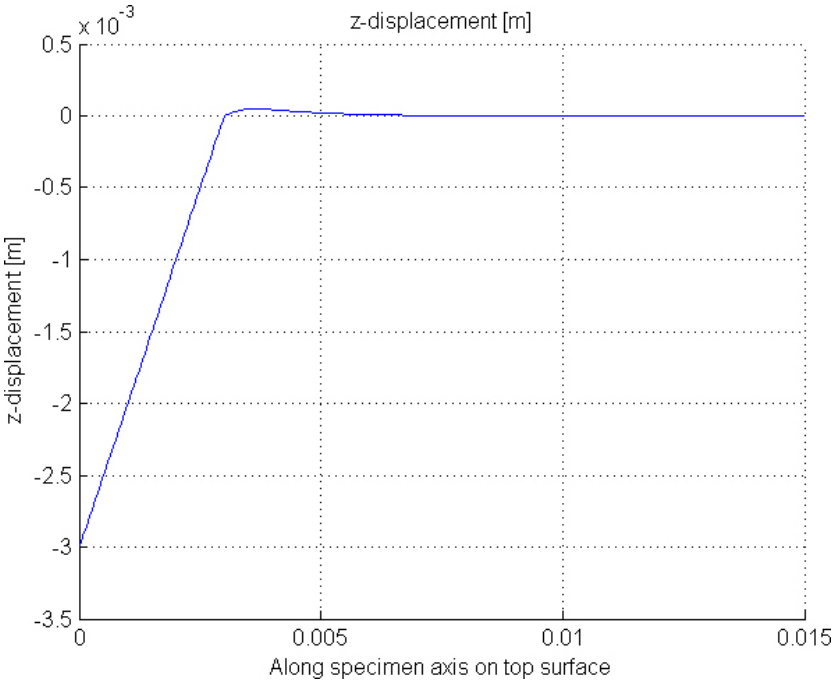


***Figure 3-2.*** *Displacement in the vertical z-direction after the indentation has been applied as a function distance from the indentation along the x-axis.*

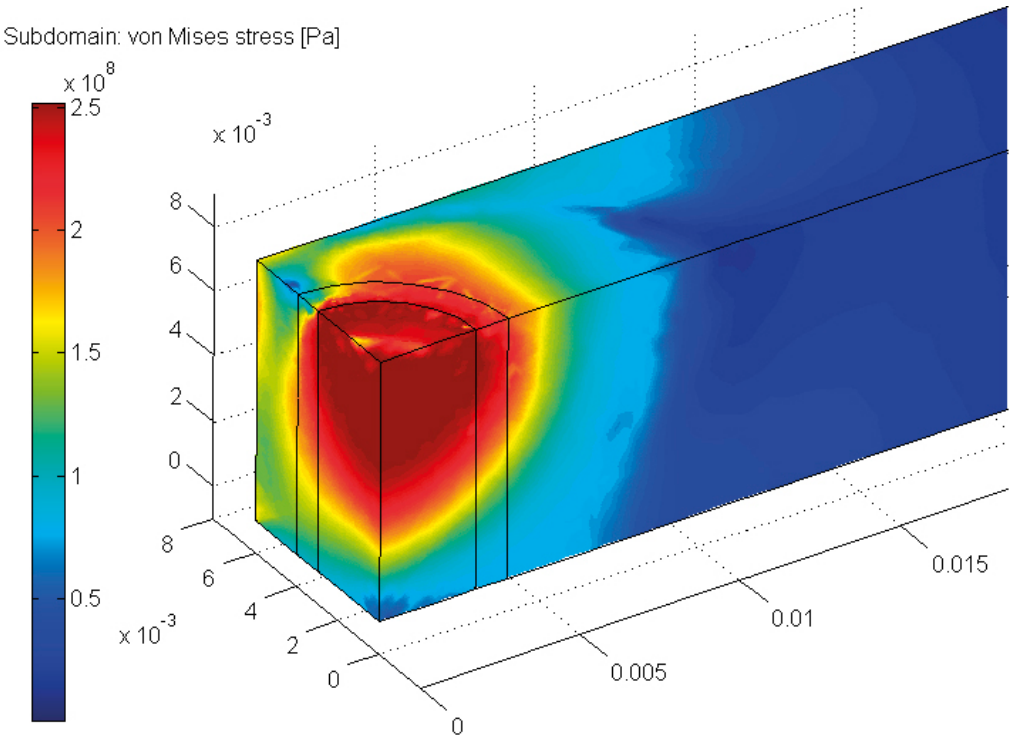


***Figure 3-3.*** *Distribution of von Mises stress in the specimen.*

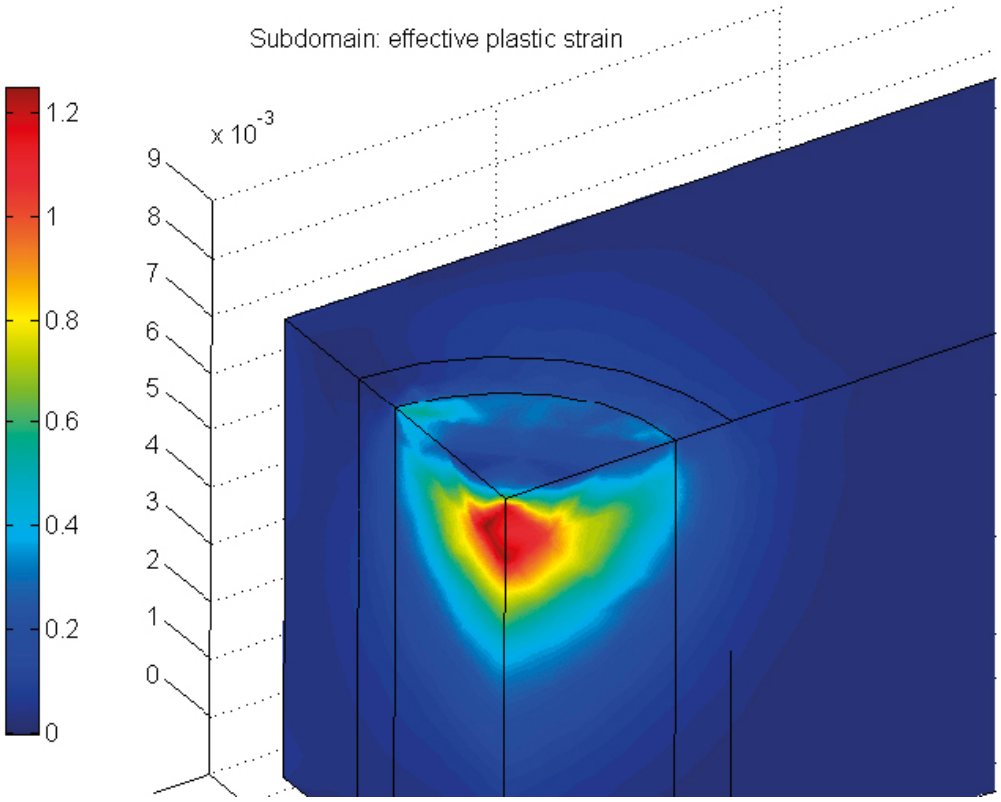


***Figure 3-4.*** *Distribution of von Mises effective strain in the specimen.*

Since only one quarter of the specimen is shown, the indenter has been inserted in the centre top corner in the figure. In the volume close to the indentation the stress is very high. The tensile strength is 250 MPa and the stress level is close to this value. The yield strength was 70 MPa. One can conclude that the specimen is plastically deformed even below the punch on the bottom side of the specimen, although only to a small extent.

At the centre of the indentation the plastic strain is very high, about 1. Strains exceeding 0.2 could have a strong influence on the creep properties (Martinsson and Andersson-Östling 2009). It is however, quite localised which should reduce its influence.

## 3.2 Indentations

As a first attempt indentation depths of 3 mm were tested. As expected from the simulations in the previous section, the specimens were fully deformed below the indenter through the thickness of the specimen. However, the observed deformation was so pronounced that a dimple formed on the backside of the specimen. This dimple was considered unacceptable since it meant that the whole of the cross sectional area was fully plasticised during the indentation. The purpose of the testing was to study assymetrical deformations and smaller indentations were thereafter used and a maximum depth of 2 mm was applied.

The indentation depths were measured using light optical microscope and an accuracy of 0.1 mm was obtained, see Table 3-1 for values of the indentation depths for all specimens. All indentations were performed at the same time and the conical body was intact, thus all indentations are similar. Figure 3-5 shows a specimen with an indentation of 1 mm.

***Figure 3-5.*** *Specimen after indentation but before creep test.*

**Table 3-1. Test matrix and creep results. The serie SKB 2A is annealed afterwards.**

| Specimen ID | Indentation depth mm | Actual stress MPa | Loading time h | Creep time h | Loading strain % | Creep strain % | Area reduction % | Min creep rate $s^{-1}$ | Comments |
|---|---|---|---|---|---|---|---|---|---|
| SKB 0-1 | 0 | 180 | | | | | | | Failure during loading |
| SKB 0-2 | 0 | 160 | 0.24 | 797 | 14.9 | 9.4 | – | 0.00179 | Interrupted |
| SKB 0-3 | 0 | 167 | 0.36 | 235 | 17.9 | 25 | 87.3 | 0.03838 | |
| SKB 0-4 | 0 | 163 | 0.37 | 1,823 | 17.4 | 17.9 | 84.5 | 0.025 | |
| SKB 0-5 | 0 | 162 | 0.29 | 3,022 | 17.2 | 30.4 | 70.8 | 0.028 | |
| SKB 1-1 | 0.9 | 161.3 | 0.34 | 810 | 26.8 | 17.1 | – | 0.00381 | Interrupted |
| SKB 1-2 | 1.04 | 168.9 | 0.37 | 111 | 20.3 | 22.8 | 86.7 | 0.07919 | |
| SKB 1-3 | 1.02 | 164.7 | 0.35 | 167 | 16.9 | 28.8 | 73.5 | 0.00726 | |
| SKB 1-4 | 1.05 | 161.8 | 0.23 | 96 | 17.2 | 33.3 | – | 0.011 | |
| SKB 1-5 | 1.01–1.03 | 161.7 | 0.23 | 1,871 | 8.8 | 38.5 | – | 0.015 | |
| SKB 15-1 | 1.56–1.58 | 164.1 | 0.24 | 644 | 15.1 | 10.9 | 21.2 | 0.001495 | Interrupted |
| SKB 15-2 | 1.51–1.52 | 171.0 | 0.28 | 389 | 17.5 | 22.7 | 83.3 | 0.02079 | |
| SKB 15-3 | 1.51–1.52 | 166.9 | 0.34 | 782 | 16.1 | 27.2 | 73.1 | 0.00923 | |
| SKB 15-4 | 1.47 | 164.6 | 0.28 | 1,785 | 19.4 | 46 | 82.4 | | |
| SKB 15-7 | 1.52 | 172.9 | 0.35 | 192 | 24.2 | 15.5 | 83.9 | 0.030949 | |
| SKB 2-1 | 1.95–1.96 | 166.5 | 0.24 | 644 | 15.2 | 19 | 23.9 | 0.0026 | Interrupted |
| SKB 2-2 | 2.01 | 174.2 | 0.35 | 297 | 17.7 | 22.6 | 85.9 | 0.03 | |
| SKB 2-3 | 2.06 | 170.4 | 0.37 | 1,080 | 15 | 22.2 | 76.5 | 0.005427 | |
| SKB 2-7 | 2.03 | 176.9 | 0.24 | 135 | 21.7 | 22.6 | 44.3 | 0.074258 | |
| SKB 2A-1 | 2 | 166.8 | 0.25 | 1,389 | 15.9 | 16 | 87.1 | 0.001517 | |
| SKB 2A-3 | 2.06–2.07 | 170.5 | 0.34 | 299 | 16.7 | 13.5 | 69.7 | 0.01232 | |
| SKB 2A-4 | 2.06 | 165.2 | 0.33 | 3,526 | 18.1 | 34.6 | 92.9 | 0.006 | |
| SKB 2A-7 | 1.99 | 172 | 0.35 | 207 | 20.3 | 16.6 | 75.3 | 0.0258 | |

## 3.3 Creep testing

The results from the creep tests are given in Table 3-1 and in graphical form in Figure 3-6 to Figure 3-13. Figure 3-6 shows actual stress versus rupture time. The actual stress is hereby standing for the effective stress on the remaining ligament after indentation and the nominal stress is the stress calculated before indentation. Specimens that were interrupted before fracture are placed within brackets. A log-log plot is used since a linear relation between creep stress and rupture time is obtained. Trend lines (interrupted specimens are not included) are added for all series to simplify interpretation. All series have a similar behaviour where rupture time increases linearly with decreasing stress.

At an actual stress around 165 MPa, the indentation depths show different behaviour. A depth of 1 mm gives a shorter rupture time, approximately 6 times shorter, compared to the reference series (no indentation). When increasing the indentation depth an increase in rupture time is seen. A depth of 1.5 mm gives about 3 times longer time before rupture. When increasing to 2 mm the rupture time increases with a factor 13 compared to the reference. For the series where the specimens have indentations of 2 mm and afterwards annealed a rupture time between 1.5 mm and 2 mm is obtained.

In Figure 3-7 the minimum creep strain rate is plotted as function of actual stress in a log-log plot, showing a linear relation were creep rate decreases with decreasing stress following the Norton power law, eqn 1. The calculated Norton exponents are listed in Table 3-2, and it is seen that the exponents are well within the power law breakdown region.

$$\dot{\varepsilon} = A_0 \exp(-\frac{Q}{RT})\sigma^n \qquad \text{(Equation 3-1)}$$

Where ε is the creep rate, $A_0$ is a material constant, $Q$ the activation energy for creep, $T$ the temperature, $R$ the gas constant, σ the stress and $n$ the Norton exponent.

The creep ductility is given in Figure 3-8 to Figure 3-11 showing loading strain, creep strain and total strain versus actual stress, respectively. Interrupted specimens are placed within brackets. When studying the loading strain all specimens have strains over 15%, except for specimen SKB 1-5. The creep strain and total strain show a scatter over all specimens and the indentation depths do not have a clear influence. One specimen without indentation and two with 2 mm indentations and afterwards annealed show the lowest creep and total strains. The creep strain is over 15% and the total strain over 30% for all specimens. Figure 3-11 shows area reduction as function of actual stress and all specimens lie between 70 and 95% in area reduction.

**Table 3-2. Calculated Norton exponents.**

| Material | Norton exponent |
|---|---|
| Annealed, no indentation | 60 |
| Annealed, 1 mm indentation | 47 |
| Annealed, 1.5 mm indentation | 54 |
| Annealed, 2 mm indentation | 59 |
| 2 mm indentation, annealed again | 49 |

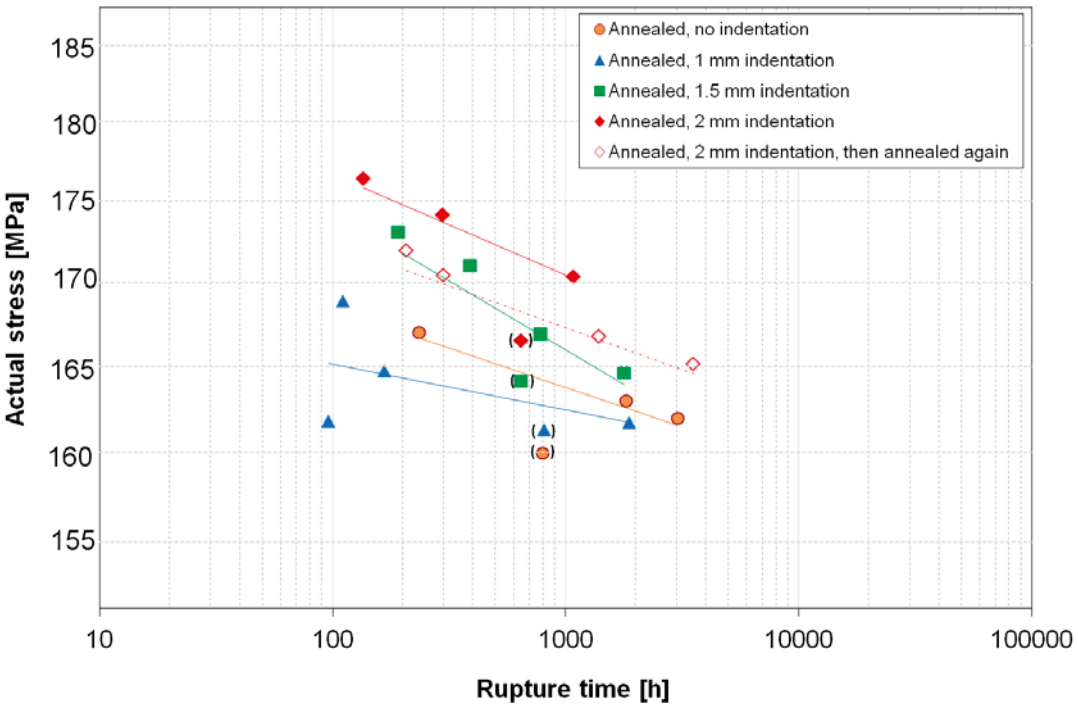


***Figure 3-6.*** *Actual stress against rupture time for all test series. Values inside parenthesis are interrupted tests. Linear trend lines are added for each series.*

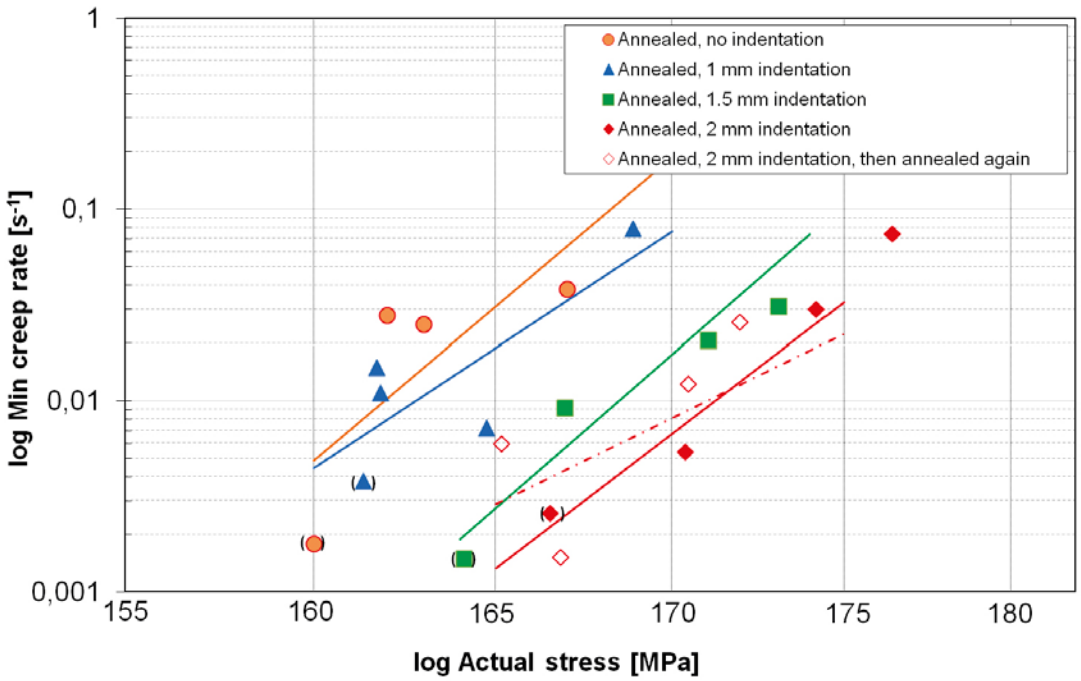


***Figure 3-7.*** *Minimum creep rate against actual stress for all test series. The slope of the trend lines is equal to the Norton coefficient.*

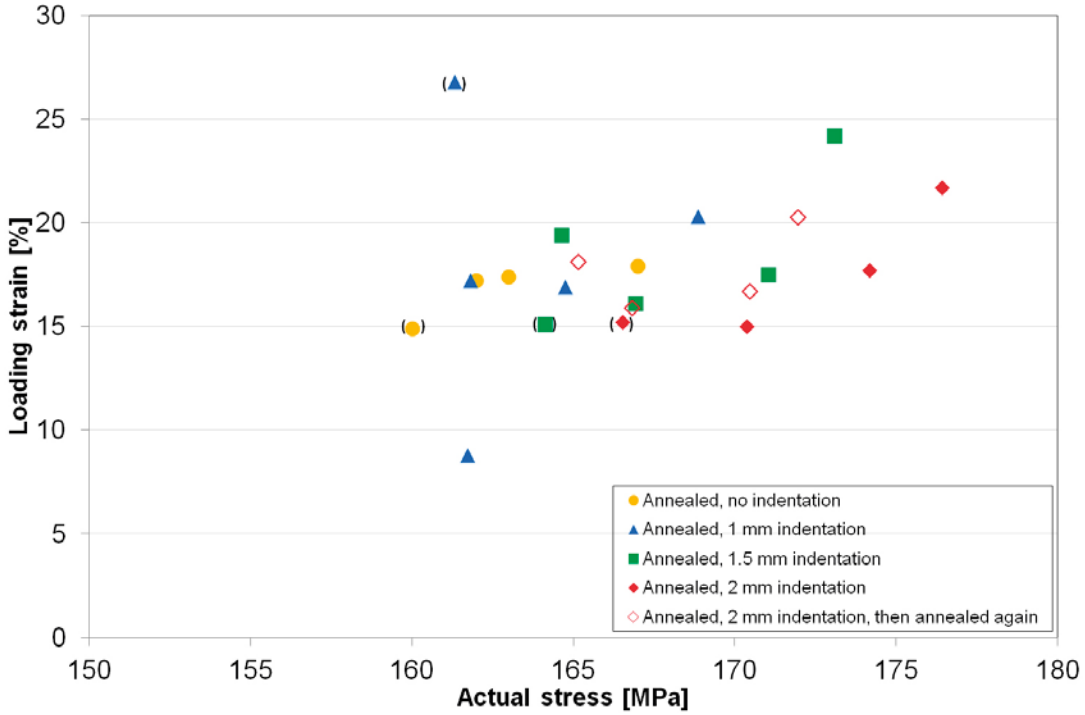


***Figure 3-8.*** *Loading strain versus actual stress for all test series. Values inside parenthesis are interrupted tests.*

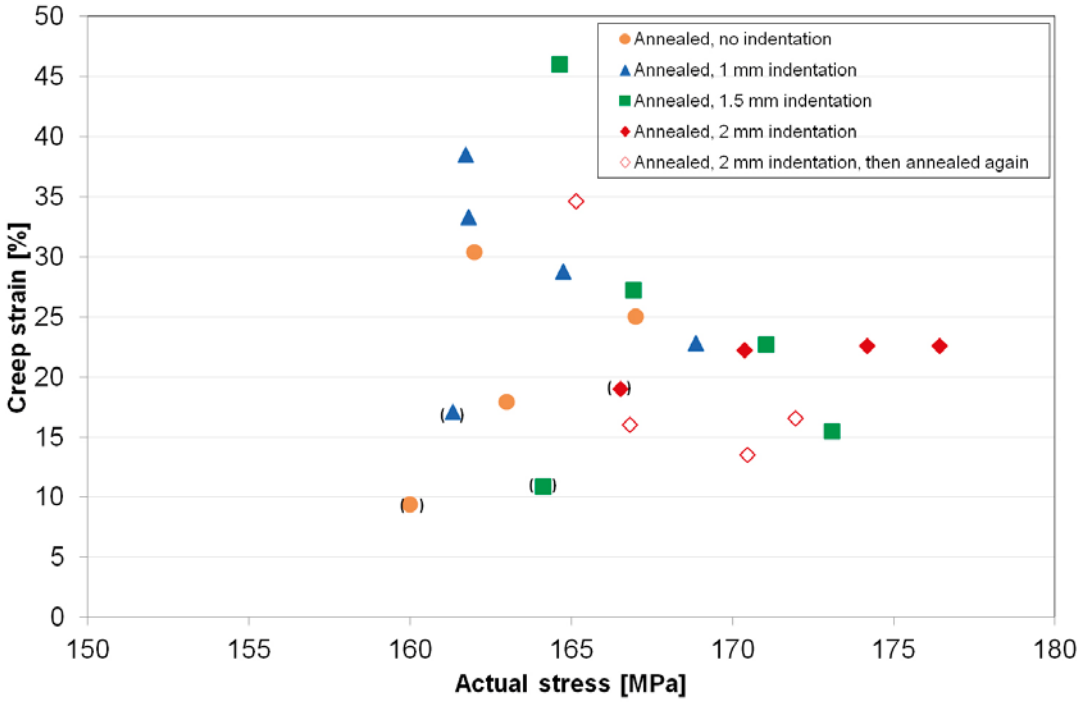


***Figure 3-9.*** *Creep strain versus actual stress for all test series. Values inside parenthesis are interrupted tests.*

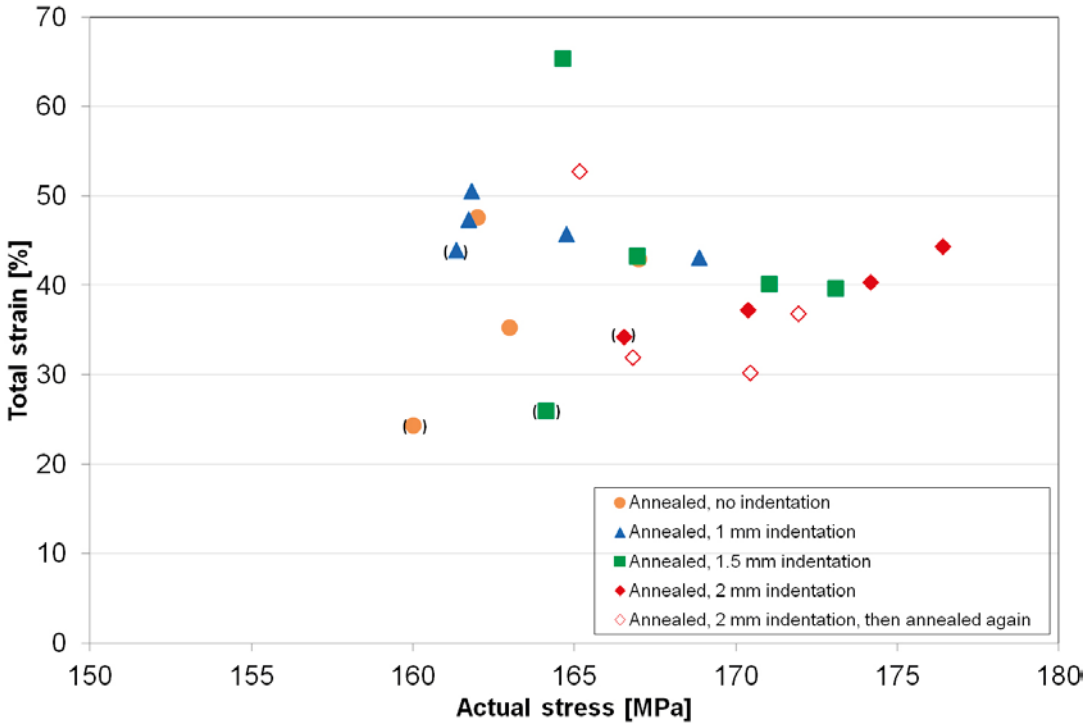


***Figure 3-10.*** *Total strain versus actual stress for all test series. Values inside parenthesis are interrupted tests.*

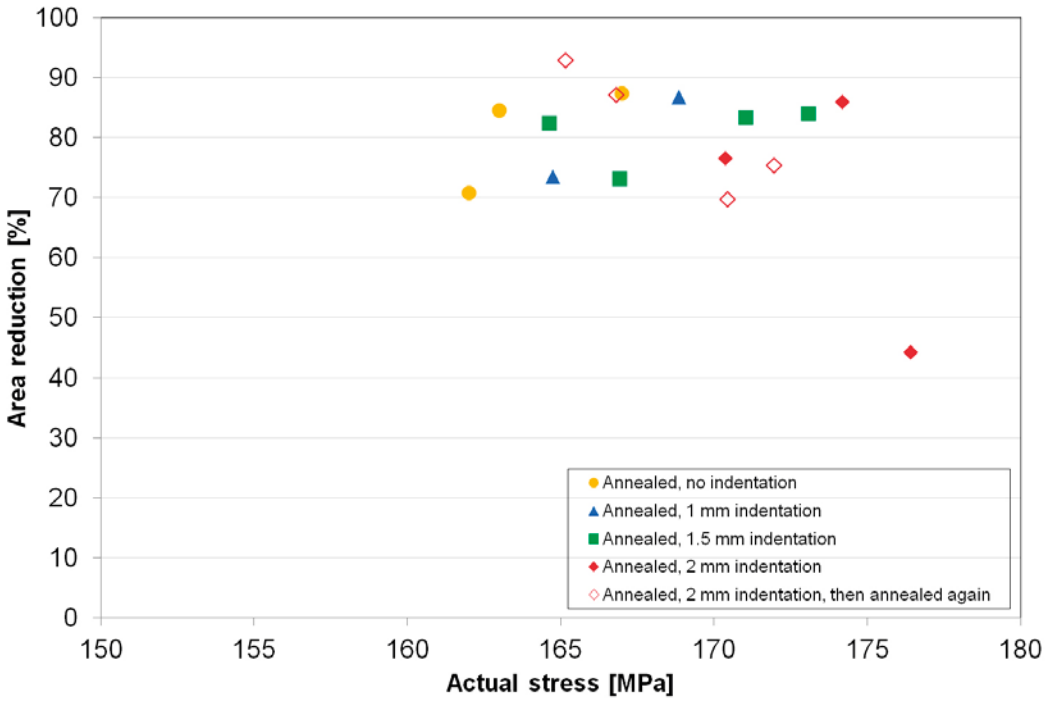


***Figure 3-11.*** *Area reduction versus actual stress for all test series.*

Figure 3-12 show creep curves for one specimen in each test series, having comparable life times. The curves show clear primary, secondary and tertiary creep stages. For the specimen 2 mm and annealed after, fracture happens very fast after entering the tertiary creep stage. When comparing creep curves having the same nominal stress, 163 MPa, no progression in life time is seen, i.e. a larger indentation does not give a shorter life time, see Figure 3-13. For the specimen with no indentation the tertiary creep stage is not reached before fracture and the secondary stage is much longer than for the other specimens. For 1 mm indentation fracture happens during secondary creep or very fast after entering the tertiary creep stage.

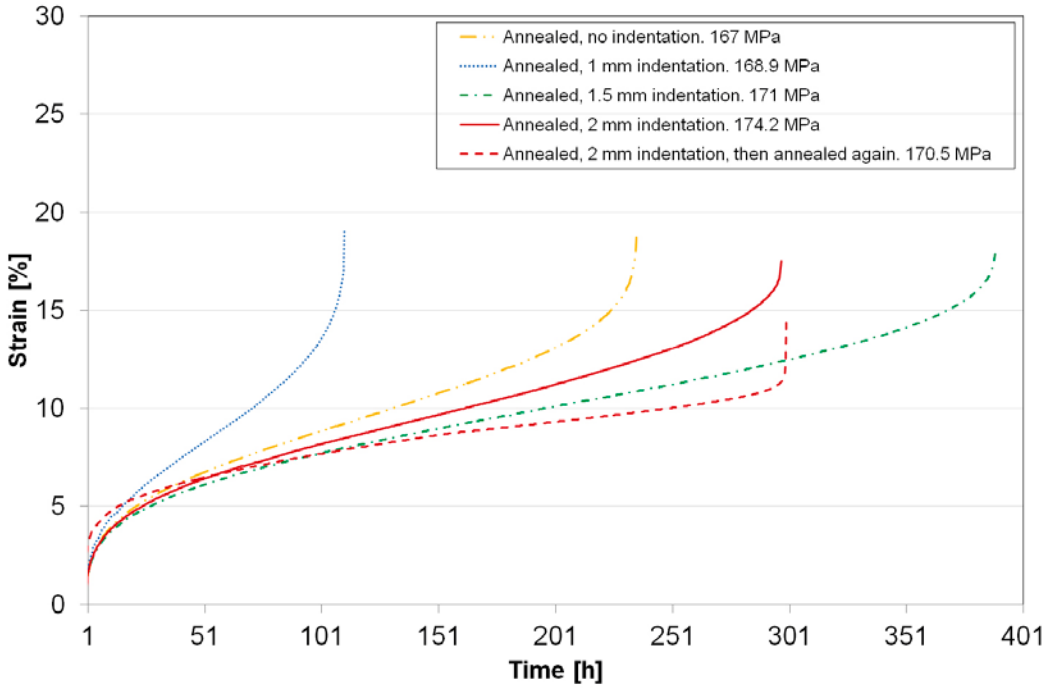


***Figure 3-12.*** *Creep curves for one specimen in each test series, having comparable life times. Actual stress for all specimens seen in legend.*

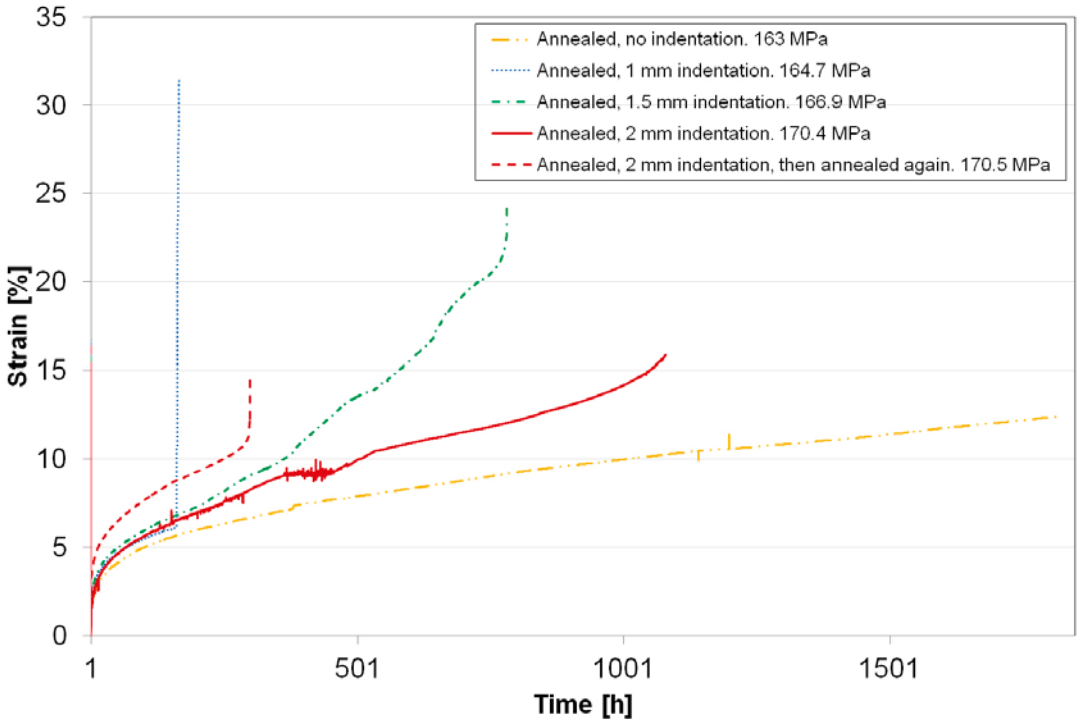


***Figure 3-13.*** *Creep curves for one specimen in each test series, have the same nominal stress, 163 MPa. Actual stress for all specimens seen in legend.*

## 3.4 Metallography

Two specimens that were interrupted before fracture were studied metallographically in macro scale. Figure 3-14 shows SKB 2-1 and SKB 15-1. It is clearly seen that slip planes are activated along the whole surface since the surface is rough. In the area near the indentations a cross can be seen, Figure 3-15, this is due to that the slip planes have favoured the 45° direction. When studying the area nearby the indentation and inside the cavity no cracks are seen and thus there is no tendency for crack propagation in the oxide due to the cold deformation. In spite of the large cold deformation the indentation on SKB 2-1 has stretched without cracking.

These results agree well with simulations of where hard and soft areas can be found.

The fracture has not always occurred in the middle of the specimen, i.e. through the indentation, instead three variants are seen, Table 3-3.

- Fracture through the indentation.
- Fracture in the deformed zone.
- Fracture outside the deformed zone.

The deformed zone is around 1.5–2 mm wide and is seen as a blister around the indentation. For all series except for the one annealed after indentation, fracture occurs in different zones, but for the series annealed after indentation the fracture always occurs through the indentation, see Table 3-3. However more tests have to be done to be able to verify this. In Figure 3-16 examples are seen showing fracture far away and through the indentation.


***Figure 3-14.*** *Image of the whole specimens.*

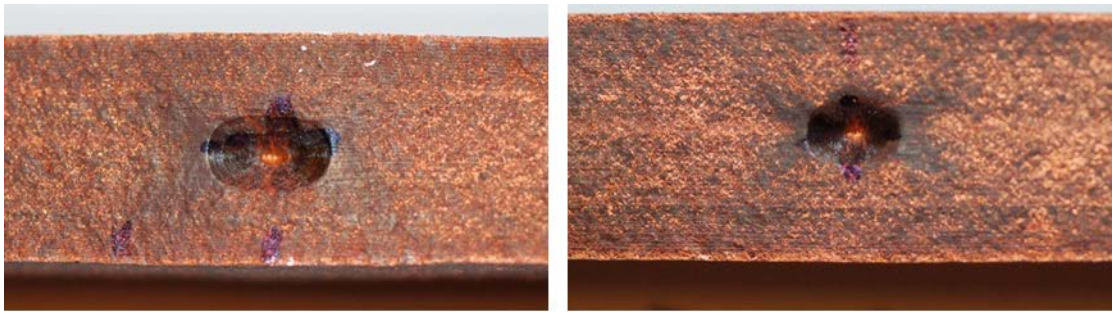

***Figure 3-15.*** *Images over the area of the indentation and cross. To the left: SKB 2-1, to the right: SKB 15-1.*

***Figure 3-16.*** *Image showing the distance from fracture to indentation. Over: SKB 2-4, under: SKB 2A-4.*

**Table 3-3. Distance from middle of indentation to fracture for all specimens.**

| Specimen ID | Distance from indentation to fracture cm |
|---|---|
| SKB 0-3 | 0.5 |
| SKB 0-4 | 0.25 |
| SKB 0-5 | 2 |
| SKB 1-2 | 3 |
| SKB 1-3 | 1 |
| SKB 1-4 | 1 |
| SKB 1-5 | 1.5 |
| SKB 15-2 | Through indentation |
| SKB 15-3 | 1.7 |
| SKB 15-4 | 2 |
| SKB 15-7 | Through indentation |
| SKB 2-2 | Through indentation |
| SKB 2-3 | Through indentation |
| SKB 2-4 | 2 |
| SKB 2-7 | Through indentation |
| SKB 2A-1 | Through indentation |
| SKB 2A-3 | Through indentation |
| SKB 2A-4 | Through indentation |
| SKB 2A-7 | Through indentation |

## 3.5 Geometry measurement

3D scanning of four specimens was performed at Swerea SICOMP and compared to the metallographic study. Figure 3-17 shows SKB 1-2, after indentation but before creep testing showing a smooth surface without variation in geometry. In Figure 3-18 SKB 2-1 is seen where the indentation shows a large effect on the geometry and a blister is seen on the middle of the specimen. The rest of the specimen shows a homogenous geometry. For SKB 2A-1, annealed after indentation, no blister is seen at the middle, Figure 3-19. A small torsion is seen, which probably is due to that the threads have slipped during straining. SKB 15-1 shows an asymmetrical deformation, Figure 3-20, where the specimen in some way has twisted.

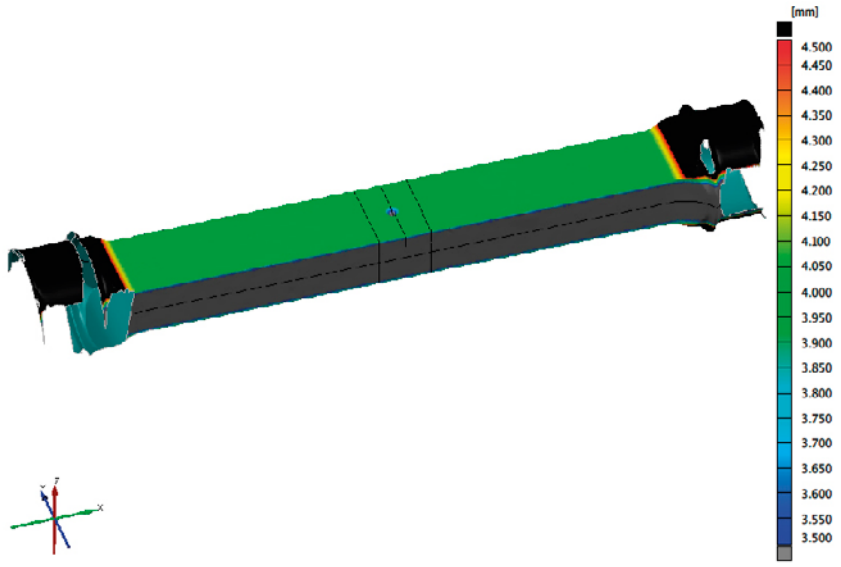


*Figure 3-17. SKB 1-2, annealed 1 mm indentation, not tested.*

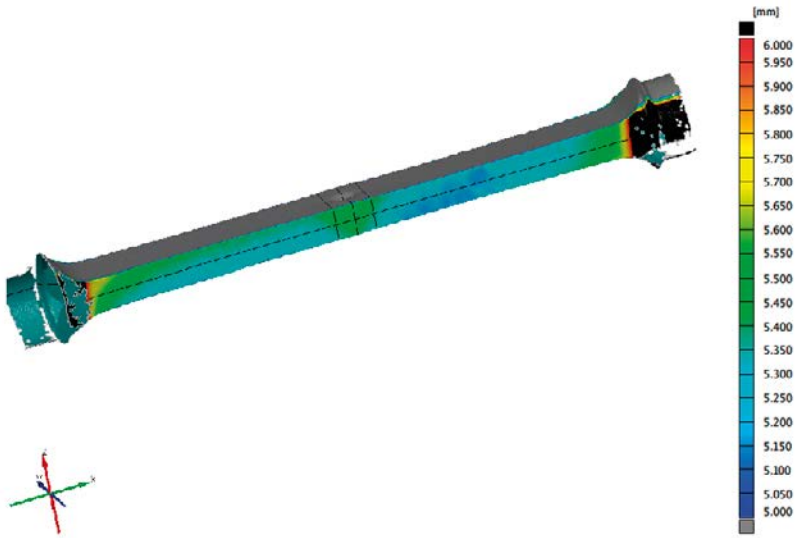


***Figure 3-18.*** *SKB 2-1, annealed 2 mm indentation.*


***Figure 3-19.*** *SKB 2A-1, annealed 2 mm indentation then annealed again.*

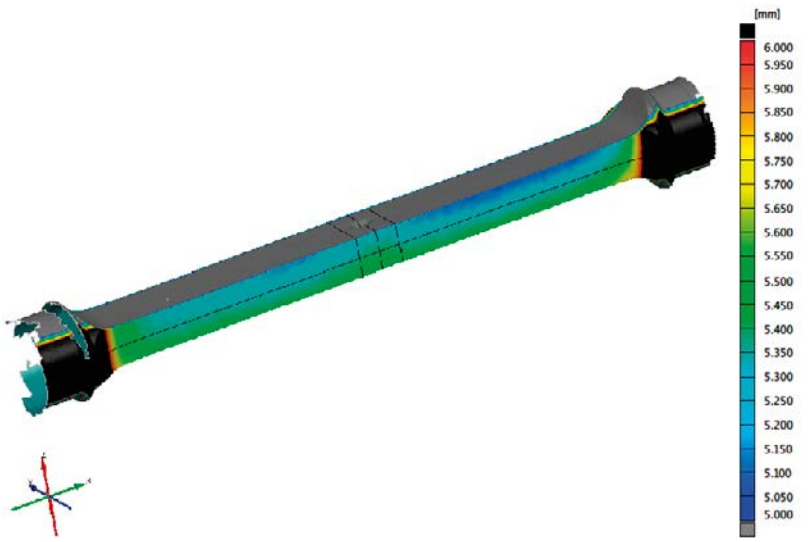


***Figure 3-20.*** *SKB 15-1, annealed 1.5 mm indentation.*

# 4 Discussion

There are some uncertainties in the results. The number of specimens in each series is not enough for definitive conclusions, however trends can be seen. The scatter in stress around the trend lines in the stress versus rupture time plot is very small except for the series "annealed, 1 mm indentation" which shows a pronounced scatter at short times, Figure 3-6. The Norton exponent is experimentally derived from the plot of minimum creep rate against stress. Here the scatter is larger and the accuracy of the Norton exponent for the two series "annealed no indentation" and "annealed 1 mm indentation" should be considered as indicatory. However, the estimated Norton coefficients are well into the power law breakdown region, and comparable to previous work (Andersson-Östling and Sandström 2009).

The loading strain is between 15 and 30% which is comparable to other creep tests using the same type of loading (Martinsson and Andersson-Östling 2009). For stress versus rupture time, no progression of the values is seen with indentation depth. All series are within the same scatter band. This differs from the study on the effect of cold work with different amount of cold work in both tension and compression which showed an increase in creep life with amount of introduced cold work in tension (Martinsson and Andersson-Östling 2009).

Earlier experiments performed on the same creep test rigs tested at the same temperature show similar results with the series annealed no indentation, see Figure 4-1 (Sandström and Hallgren 2012). It is evident that the results are slightly lower but in the scattering band of the slow loading tests. One difference between the two studies is that in the slow loading tests study, different loading rates were used and in this study the same loading rate is used for all specimens (Sandström and Hallgren 2012).

FEM simulations show that the deformed zone around the indentation both becomes wider and deeper with increasing size of indentation. However the experiments do not show any clear behaviour in where the fracture occurs, through the indentation, in the deformed zone or outside the deformed zone, for different indentation depths.

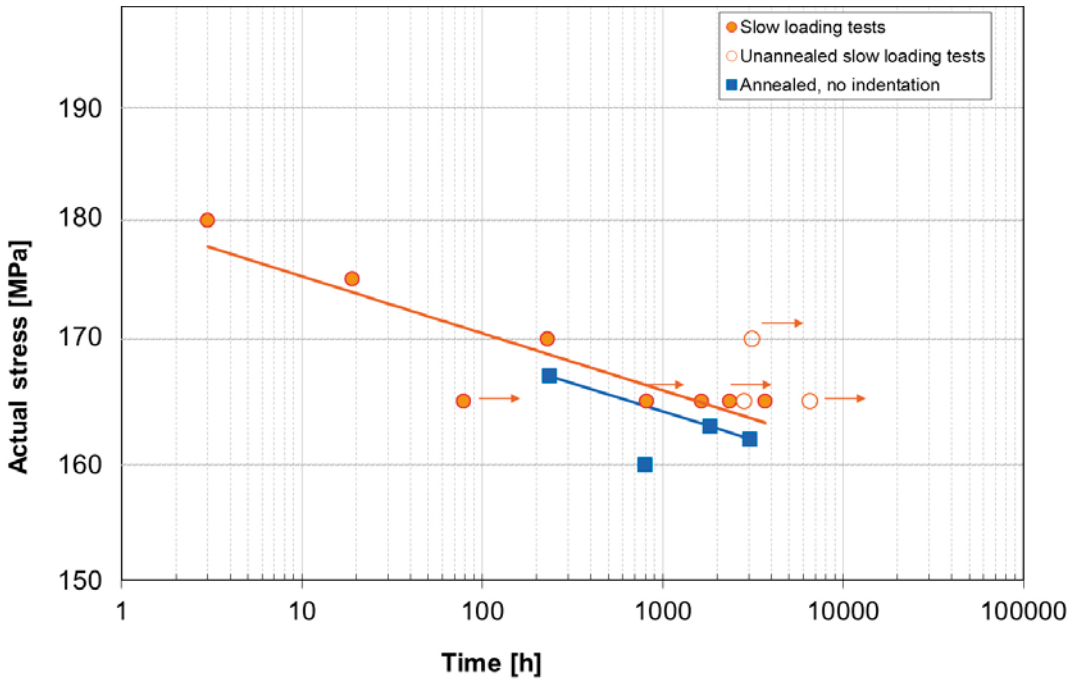


***Figure 4-1.*** *Actual stress versus time for the series "annealed no indentation" compared with slow loading tests.*

The specimens show necking on both sides of the indentation with a blister in the middle. Close to the indentations the material has work hardened and the material does not creep as fast as far away from the indentation and the necking has been held back. With increasing cold deformation the specimen becomes harder and the work hardened area around the indentation increases and larger blisters are seen on the specimens. For the specimens annealed after indentation, this phenomenon is not seen and they are comparable with the specimens without indentations. When studying SKB 2-1 the indentation is stretched which probably is due to that the slip planes neutralise the cold deformation and the material is ductile even on places where there was large cold deformation. Figure 4-2 shows a exaggerated drawing of the general appearing of necking, blister, slip planes and the cold deformation "bubble" in the specimen.

Fracture occurs at different distances from the indentations and when the fracture has occurred through the indentation the cold deformation has been very large so that the ductility under the indentations is lowered and the material is brittle and the fracture occurs through the indentation even if brittle fracture is not seen.

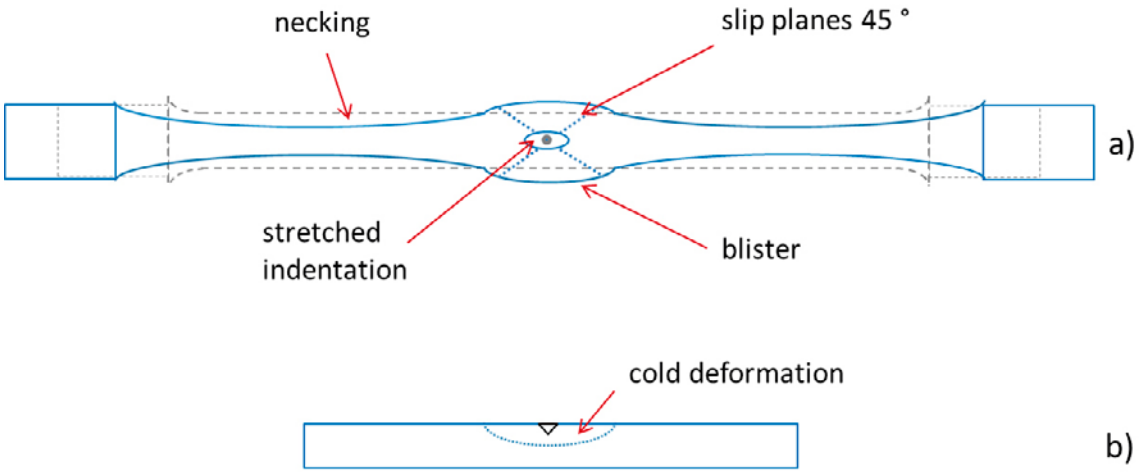


***Figure 4-2.*** *a) Schematic drawing showing the necking, slip planes and blister b) cold deformation"bubble".*

# 5 Conclusions

Creep tests of flat specimens with local cold work introduced with a conical punch have been performed. Three indentation depths 1, 1.5, and 2 mm were studied giving increasing amount of cold work. A reference series without indentation was also included. There are some uncertainties in the results. The number of specimens in each series is not enough for definitive conclusions, however trends can be seen.

- The rupture time and creep ductility (elongation) of the tests were not markedly influenced by the indentation, i.e. the amount cold work in spite of the fact that FEM simulations demonstrate that most of the section near the indentation was plastically deformed.
- The total strain at rupture, i.e. the loading strain plus the creep elongation was 30 to 65%.
- A significant influence of the indentation was that the minimum creep rate was reduced with increasing amount cold work. This is consistent with previous creep tests on cold deformed copper. Around the indentation the creep deformation was also lower than in the rest of the gauge length.
- No cracks were found in the area near the indentation or inside the indentation cavity.
- According to FEM-simulations the local true plastic strain around the indentation can be as high as 1. From the experiments it is evident that this has no negative effect on the creep behaviour and in particularly not on the creep ductility. The reason is that the volume around the indentation forms a local creep hard region and much of the creep deformation takes place outside this volume. This makes the copper material “forgiving” with respect to local indentations.

# Acknowledgment

Svensk Kärnbränslehantering AB is gratefully acknowledged for funding this work and supplying the test material. We would also like thank Facredin Seitisleam for help with the experiments and Åsa Martinsson for valuable discussions and help with the work.

# References

SKB's (Svensk Kärnbränslehantering AB) publications can be found at www.skb.se/publications. References to SKB's unpublished documents are listed separately at the end of the reference list. Unpublished documents will be submitted upon request to document@skb.se.

**Andersson-Östling H C M, Sandström R, 2009.** Survey of creep properties of copper intended for nuclear waste disposal. SKB TR-09-32, Svensk Kärnbränslehantering AB.

**Martinsson Å, Andersson-Östling H C M, 2009.** Effect of cold work on creep properties of oxygen-free copper. Technical Report KIMAB-2009-109, Swerea KIMAB.

**Sandström R, Hallgren J, 2012.** The role of creep in stress strain curves for copper. Journal of Nuclear Materials 422, 51–57.

**SKB, 2010.** Design, production and initial state of the canister. SKB TR-10-14, Svensk Kärnbränslehantering AB.

#### Unpublished documents

| SKBdoc id, version | Title | Issuer, year |
|---|---|---|
| 1205273 ver 2.0 | Intryck i koppar. (In Swedish.) | SKB, 2009 |